Polycrystalline Formamidinium Lead Bromide X-ray Detectors

Suad Alghamdi, et al.

Supplementary Information

X-ray Absorption and Photocurrent

In Figure 1 the total mass attenuation coefficient is calculated as a function of photon energy using the NIST XCOM database [Ber10]. The mass attenuation coefficient is calculated from the atomic composition of the compound, eg. where $FAPbBr_3$ has a composition of $CN_2H_5PbBr_3$.

The incident photon flux Φ_0 over an area A is related to the X-ray dose rate in air, D, by:

$$D = \left(\frac{\mu}{\rho}\right)_{air} \frac{\phi_0 \, E_X \, q}{A} \tag{S1}$$

where E_x is the average energy per X-ray photon (in eV). Therefore the photon flux incident on the detector is given by:

$$\phi_0 = \frac{DA}{\left(\mu/\rho\right)_{air} E_X \, q} \tag{S2}$$

For an X-ray detector the intrinsic detection efficiency ε_{INT} is defined as [Kno00]:

$$\varepsilon_{INT} = \frac{number \; of \; pulses \; recorded}{number \; of \; photons \; incident \; on \; detector} \tag{S3}$$

which can be approximated by the relative X-ray absorption ε_X where:

$$\varepsilon_X(x) = 1 - \frac{\phi(x)}{\phi_0} = 1 - e^{-\frac{\mu}{\rho}\rho x} \tag{S4}$$

where $\frac{\mu}{\rho}$ is the total mass attenuation coefficient of the detector material summed across all photon interaction processes, ρ is the material density, x is the detector thickness, and $\phi(x)$ is the photon flux after passing through material of thickness x.

In order to estimate the magnitude of the signal current from the X-ray detector, knowledge is required of the charge collection efficiency η which is defined as the fraction of the generated electron/hole pairs that contribute to the measured signal [Aku69]. In a detector material with good charge transport, such as silicon, the charge collection efficiency $\eta \sim 1$. For perovskite materials where the carrier drift length is less than the detector thickness, the charge collection efficiency can be estimated from the average carrier mobility and lifetime, such that:

$$\eta = \frac{measured \; charge}{generated \; charge} \approx \frac{\mu\tau \, E}{d} \tag{S5}$$

where μ is the carrier mobility, τ the carrier effective lifetime, E the electric field strength in the device, and d is the material thickness.

The generated photocurrent I_X is given by

$$I_X = \eta\phi\beta q \qquad (S6)$$

where β is the number of electron/hole pairs generated in the detector material per deposited energy. This value is determined by the electron/hole pair creation energy, commonly referred to as W, such that

$$\beta = \frac{E_X}{W} \qquad (S7)$$

and W is estimated from ~2.7x the material bandgap based on the approach of Klein et al. [Kle68].

Influence of Escape Peaks

Generally X-ray detectors will exhibit X-ray escape photons, due to the escape from the detector volume of characteristic X-rays produced from the constituent atoms. For detectors fabricated using high-Z materials, the resulting higher characteristic X-ray energies can lead to the presence of more significant escape photons. In a spectroscopic photon-counting detector, the presence of one or more escape peaks can often be observed below the main photo peaks.

Table S1 presents the total mass attenuation coefficient, and the mean photon attenuation length for 100 keV photons, calculated for CdTe and also for FAPbBr$_3$ using NIST XCOM [Ber10]. In both materials, a X-ray energy of 100 keV is significantly above the dominant K-shell ionisation edges. It can be seen that the mean attenuation length at 1.0mm for CdTe and 0.9mm for FAPbBr$_3$, is quite similar in both materials. However the K-shell X-ray (fluorescence) yield is 14% higher for FAPbBr3 (ω_k = 0.97) compared to CdTe (ω_k = 0.85).

Using GEANT4 Monte Carlo [Ago03], the percentage of K-shell escape events is also estimated, for 100 keV photons incident on material with a thickness of 1mm. The K-shell X-ray yield ω_k, defined as the fraction of atoms that decay by emitting a K-shell X-ray, is 14% higher for FAPbBr$_3$ compared to CdTe, and the fraction of K-shell escape events for 100 keV incident photons is 75% greater. In contrast, for X-ray energies below ~75 keV the effect of K-shell escape events from FAPbBr$_3$ is significantly reduced.

Material	Total Mass Attenuation Coefficient (cm^2/g) @ 100 keV	Mean attenuation length (mm) @ 100 keV	K-shell X-ray yield ω_k	% K-shell escape events, for 100 keV incident X-rays (1mm thickness)
CdTe	1.67	1.0	0.85	36%
FAPbBr$_3$	2.69	0.9	0.97	63%

Table S1: Summary of mean attenuation length and K-shell escape peaks, calculated using NIST XCOM and GEANT4 Monte Carlo.

X-ray tube energy spectrum

Figure S1 shows the X-ray energy spectrum of the X-ray tube used in this work, which is the Amptek Mini-X2 fitted with a gold target [Amp22]. This gives a broadly flat X-ray emission spectrum for energies above the Au L-series emissions. No additional filtering was applied to the X-ray tube. All the X-ray sensitivity measurements were carried out at 40 kV, below the Pb K-shell edge energy.
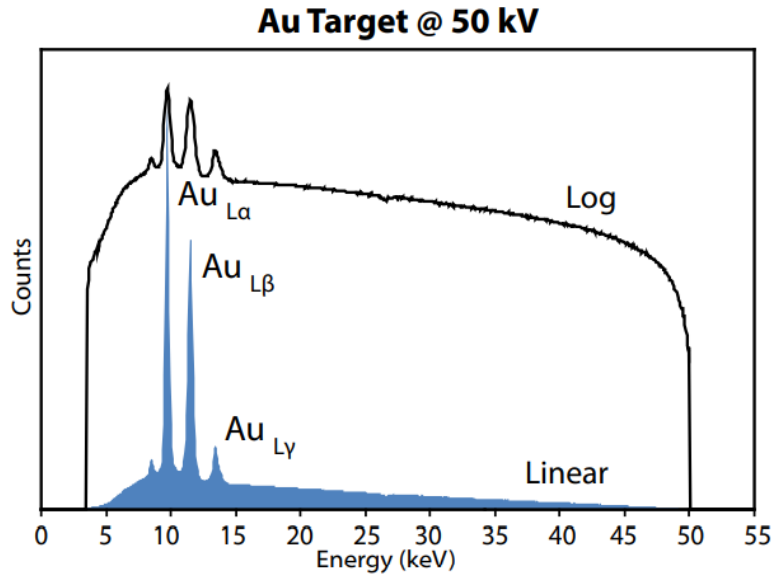

Figure S1: X-ray energy spectrum of the Amptek Mini-X2 X-ray tube [Amp22].

X-ray Sensitivity

The X-ray sensitivity *S* for a photocurrent detector is defined as

$$S = \frac{1}{A}\frac{\Delta(I_x - I_{dark})}{D}$$

where *A* is the sensitive area of the detector, I_x is the device X-ray photocurrent, I_{dark} is the device dark current, *D* is the dose rate (Gy air kerma per second).

Experimental Error Estimates

Pellet density was calculated by measuring the thickness of the pellet with a micrometer, and weighing its mass. The dominant error was in the thickness measurement, estimated at +/-0.1mm or approx. +/-4% as shown in Figure 2(b).

Current measurements were carried out in a low noise screened enclosure, with a typical point-to-point variation of +/-10 pA. Each data point is the average of 10 identical measurements sampled by the acquisition computer. The random precision on each current measurements is therefore <10 pA and the error bars are too small to show on the data points in Figures 5a and 6a.

Influence of pellet annealing

Figure S2 shows the increase in X-ray sensitivity due to annealing of the pellet in air at 145°C for 15 minutes. For the pellets pressed at 12 MPa there was a strong increase of ~150% in X-ray sensitivity as a result of annealing, with a much smaller corresponding increase for the 24 MPa pellet.
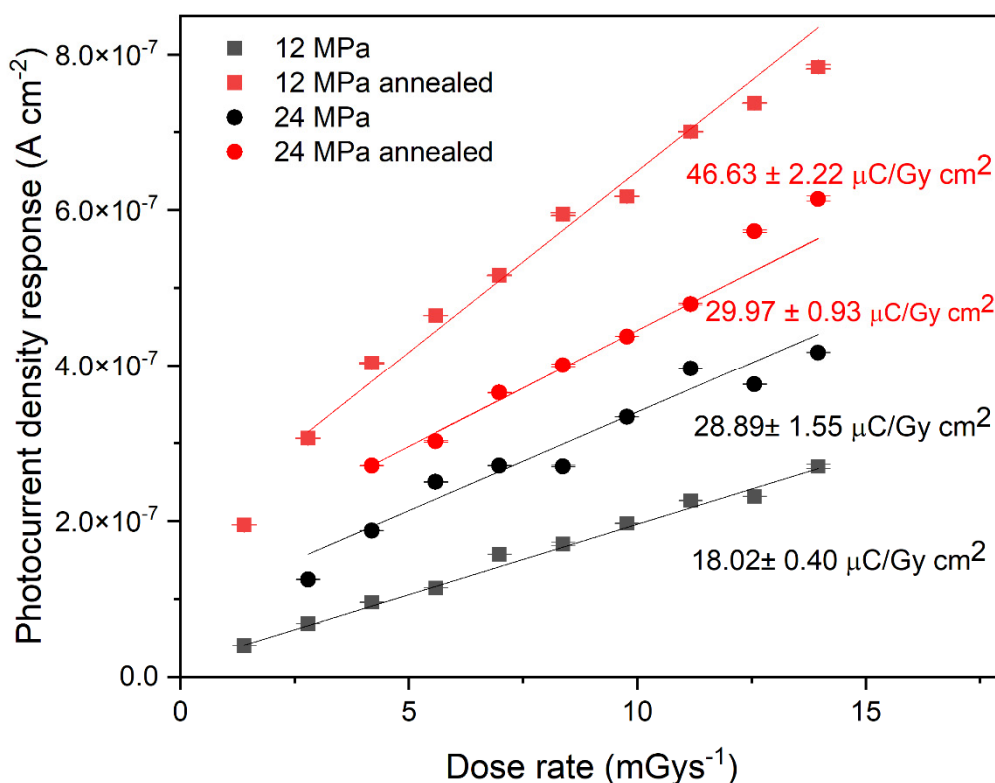

Figure S2: Influence of pellet annealing on the measured X-ray sensitivity.

References

11. [Ber10] M. Berger et al., "Photon Cross Sections Database, NIST Standard Reference Database, PML, Radiation Physics Division 2010". doi:https://dx.doi.org/10.18434/T48G6X.

14. [Kno00] G.F. Knoll, Radiation Detection and Measurement, 4th Edition, Wiley 2000, New York USA.
https://www.wiley.com/en-us/Radiation+Detection+and+Measurement,+4th+Edition-p-9780470131480

13. [Aku69] Akutagawa, W., et al., "Gamma response of semi-insulating material in the presence of trapping and detrapping," Journal of Applied Physics **40**: 3838-3854.

15. [Kle68] C.A. Klein, "Bandgap Dependence and Related Features of Radiation Ionization Energies in Semiconductors", J. Applied Physics **4** (1968) 2029-2038.

12. [Ago03] S. Agostinelli et al., "Geant4 - A Simulation Toolkit", Nucl. Instrum. Meth. A 506 (2003) 250-303.

21. [Amp22] Technical specification of 'Mini X2' Miniature X-Ray Source, Amptek Inc, Bedford MA, USA. www.amptek.com downloaded January 2022.